pagepress

Geospatial Health 2022; volume 17(s1):1083

Global spreading of Omicron variant of COVID-19

Pengxin Zhang,[1,2] Shuhan Yang,[1,2] Shaoqing Dai,[2,3] Darren How Jin Aik,[1,2] Shujuan Yang,[4,2] Peng Jia[1,2]

[1]School of Resource and Environmental Sciences, Wuhan University, Wuhan, China; [2]International Institute of Spatial Lifecourse Health (ISLE), Wuhan University, Wuhan, China; [3]Faculty of Geo-information Science and Earth Observation, University of Twente, Enschede, the Netherlands; [4]West China School of Public Health and West China Fourth Hospital, Sichuan University, Chengdu, China

Abstract

Although two years have passed since the coronavirus disease 2019 (COVID-19) outbreak, various variants are still rampant across the globe. The Omicron variant, in particular, is rapidly gained dominance through its ability to spread. In this study, we elucidated the spatial distribution pattern of Omicron from a global perspective. We used the cumulative number of notified COVID-19 cases per country spanning four weeks up to February 10, 2022, and the proportion of the Omicron variant genomic sequences from the Global Initiative on Sharing Avian Influenza Data (GISAID). The global spatial distribution of Omicron was investigated by analyzing Global & Local Moran's *I* and Getis-Ord General G. The spatial weight matrix was defined by combining K-Nearest neighbour and flight connectivity between countries. The results showed that the epidemic is relatively severe in Europe, countries with a high number of Omicron cases and incidence tended to be clustered spatially. In contrast, there are relatively fewer Omicron cases in Asia and Africa, with few hotspots identified. Furthermore, some noted spatial outliers, such as a low-value area surrounded by high-value areas, deserve special attention. This study has improved our awareness of the global distribution of Omicron. The findings can provide helpful information for deploying targeted epidemic preparedness for the subsequent COVID-19 variant and future epidemics.

Correspondence: Peng Jia, School of Resource and Environmental Sciences, Wuhan University, Wuhan, China.
E-mail: jiapengff@hotmail.com

Acknowledgements: this study was supported by the International Institute of Spatial Lifecourse Health (ISLE) and Wuhan University Specific Fund for Major School-level Internationalization Initiatives (WHU-GJZDZX-PT07).

Contributions: PZ and SY contributed equally.

Received for publication: 23 February 2022.
Revision received: 11 June 2022.
Accepted for publication: 11 June 2022.

Geospatial Health 2022; 17(s1):1083
doi:10.4081/gh.2022.1083

Introduction

Coronavirus disease 2019 (COVID-19) is a new infectious disease caused by the severe acute respiratory syndrome coronavirus 2 (SARS-CoV-2), a RNA viruses, which enters through the respiratory system with fever and cough as the main clinical manifestations. However, extrapulmonary manifestations are common in vulnerable patients (Wang *et al.,* 2020). It is the most severe public health crisis since the Spanish flu a hundred years ago. As of July 2, 2022, according to the World Health Organization (WHO), over 545 million confirmed cases and over 6.3 million deaths had been reported globally. Moreover, as with all RNA viruses, COVID-19 is also undergoing constant changes, producing many mutant strains (Kannan *et al.,* 2022). The hazards of these variants greatly enhance and manifest a rise in transmissibility, virulence, change in clinical presentation and commonly diagnostic failure resulting in a significant decline in the effectiveness of the healthcare and social measures (Alkhatib *et al.,* 2021). The SARS-CoV-2 variants include B.1.1.7 (Alpha), B.1.351 (Beta), P.1 (Gamma), B.1.617.2 (Delta), and, the most recently detected, B.1.1.529 (Omicron), which has been the least studied.

The Omicron variant was first reported on November 24, 2021 in South Africa (Callaway *et al*., 2021). According to the U.S. Centers for Disease Control and Prevention (CDC), the Omicron variant has at least 50 mutations, including more than 30 amino acid substitutions in the receptor-binding spike protein - the main vaccine target. As a result, Omicron's immune escape ability is very different from that of its predecessors (CDC, 2021; Zhang *et al.,* 2022). Specifically, three mutations, N440K, T478K, and N501Y, increase Omicron's rate of infection (Chen *et al.,* 2022). Omicron's transmission speed is alarming; it quickly replaced Delta as the previous dominant variant.

To our knowledge, using geo-spatial analysis to investigate the spatial pattern of COVID-19 incidence can indicate the magnitude and impact of the pandemic, help model and predict disease evolution and provide decision-making support for governments (Islam *et al*., 2021). A review summarized the research on geographical and geo-spatial analysis in understanding locations and the spatial patterns of COVID-19, revealing the evolution of the COVID-19 phenomenon (Franch-Pardo *et al.,* 2020) and a study has tracked changes in the spatial patterns of confirmed COVID-19 cases in Sichuan, China over the epidemic course of the infec-

tion (Jia *et al.,* 2022). Another study predicted the spatiotemporal spread of COVID-19 based on geolocated Twitter data as indicator of human movement (Bisanzio *et al.,* 2020). A similar study examined spatial cluster patterns of COVID-19 in China (Li *et al.,* 2020). To date, studies evaluating the spatial spread of the Omicron variant in the whole world remain limited. In this study, we examined spatial clustering patterns of the Omicron variant of COVID-19 at the country level to better understand the outbreak patterns and thus guide local health authorities with regard to deploying epidemic preparedness.

Materials and methods

Study site

This study was performed with 192 countries covering all continents. Data of country-based Omicron cases were estimated using the number of new confirmed cases worldwide from the Johns Hopkins University Coronavirus Resource Center, USA (https://coronavirus.jhu.edu/map.html) and the proportion of genes sequenced for the Omicron variant provided by the Global Initiative on Sharing All Influenza Data (GISAID) (2022). It should be noted that the data spans four weeks up to February 10, 2022, and the data provided by GISAID contains only 146 countries. For 46 countries where GISAID did not provide a proportion of genetic sequencing, we considered the average proportion of each country in relation to the continent it belongs to (North America 98.3%, Africa 97.4%, Oceania 95.4%, South America 93.2%, Europe 91.2%, and Asia 86.4%). We did so as the Omicron epidemic proportion in each country has been shown to be a strong indicator of new cases in that country (Tiecco *et al*., 2022). Additionally, global airline flights data we recollected from tripnoter.cn (https://www.tripnoter.cn/). This dataset, including the countries of origin and destination determines the potential, cross-border transmission points of the Omicron variant. Figure 1 shows the top five routes with the highest number of flights per country.

Statistics

This study, using the number of Omicron cases and incidence, analyzed the extent of Omicron variant development and spatial distribution of Omicron variant in countries around the world. Spatial clustering analysis with Omicron cases and incidence was conducted at the country level. Global Moran's *I* (Moran, 1950) and Getis-Ord General G (Getis and Ord, 2010) were applied to describe the general spatial distribution pattern. Global Moran's *I* indicates spatial autocorrelation, which informs whether or not the spatial distribution is random. A positive value of Global Moran's *I* at $P<0.05$, indicates the presence of clustering and negative value dispersed pattern. Getis-Ord General G can further identify whether the cluster pattern consists of high values or low values.

Local spatial statistics, including Anselin Local Moran's *I* and Getis-Ord Gi*, were employed to capture spatial patterns of Omicron variant and the location of clusters. Local Moran's *I* can identify the clusters and outliers and categorize them into four types: The High-Low (HL) outcome describes a high value surrounded by low values and the Low-High (LH) pattern a low value surrounded by high values (Anselin, 2010). High-High (HH) and Low-Low (LL) represent clusters with high or low-values, respec-

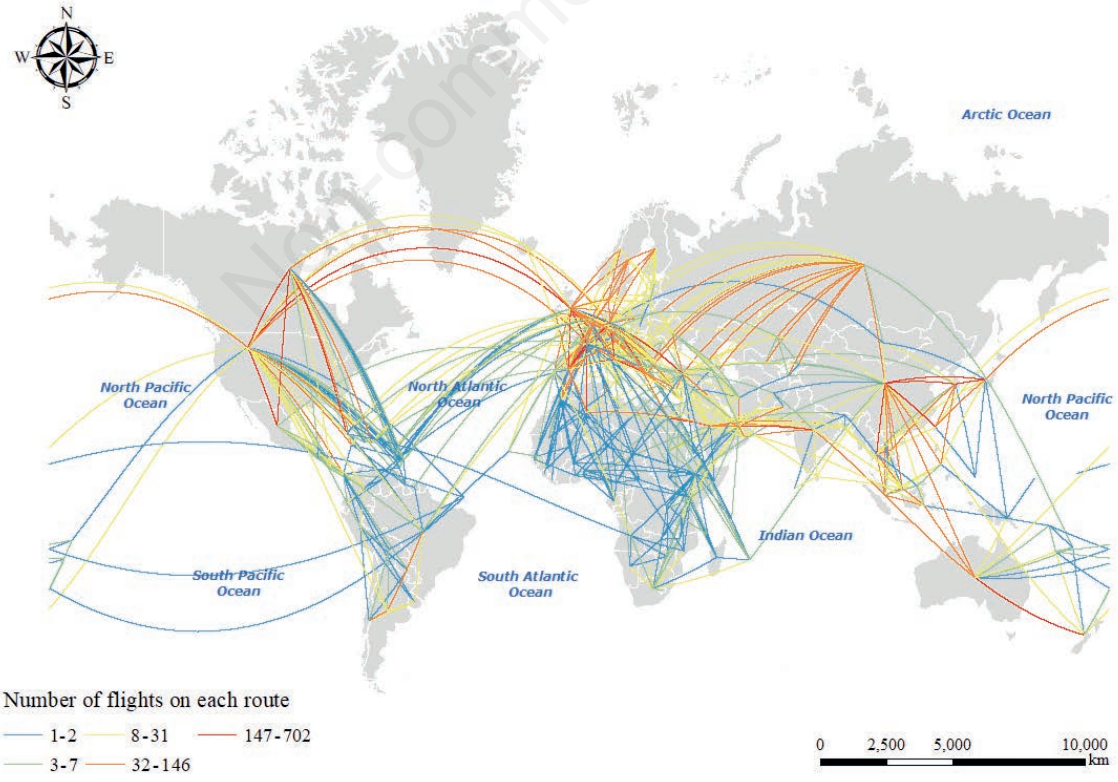

Figure 1. The top-5 routes with respect to the number of flights per country.

tively, while HL and LH are termed outliers. Getis-ord Gi* is also a local cluster commonly called hotspots analysis. It can identify hotspots (high-value clusters) and coldspots (low-value clusters) with different levels of confidence (Getis and Ord, 2010).

As a critical component of spatial clusters analysis, the spatial weight matrix in this study was defined by combining a non-parametric supervised learning method, the k-Nearest Neighbors (Fix and Hodges, 1951) with the flight connectivity between countries. Population mobility is a critical factor concerning infectious diseases transmission (Gushulak and Macpherson, 2000). The number of airlines was used to describe the population movements between countries since air travel was considered a major mean of infection spread (Findlater and Bogoch, 2018). We assigned the weights according to the normalized value of global airlines as follows:

$$W_{Aij} = n_{ij} / \sum_{m=1}^{M} n_{im} \quad (1)$$

where W_{Aij} is the weight; n_{ij} the number of flight routes between country i and j; m the number of countries where country i has direct route access.

To avoid subjective arbitrariness in setting the spatial weight matrix and to emphasize the robustness of the estimation results with different spatial weight selections, we used a nested spatial weight matrix according to Case *et al.* (1993) containing both the k-Nearest Neighbours method and flight connectivity as follows:

$$W_{ij} = \varphi * W_{Aij} + (1 - \varphi) * W_{kij} \quad (2)$$

where W_{ij} is the final weight between country i and j; W_{Kij} the weight of the k-Nearest Neighbor; and j the coefficient that takes values between 0 and 1. The closer j is to 0, the more the spatial weight is related to geographical adjacency, the closer to 1, the more the spatial weight is related to flight connectivity. The value of K (the number of the nearest neighbours) and j were determined by maximizing Moran's I (Kooijman, 1976; Ping *et al.,* 2004). In this study, K was finalized as 8 and j is finalized as 0.2.

The production of spatial weight matrix was coded in the Python programming language, vesion 3.8; spatial clustering analysis and visualization were conducted in ArcGIS, version 10.2 (ESRI, Redlands, CA, USA).

Results

Overview data

Europe and the Americas were heavily affected by the Omicron variant in the past four weeks. The highest numbers of Omicron cases (Figure 2) were seen in USA (13,007,600), France (7,877,336), India (5,954,008), and Brazil (4,313,373), while

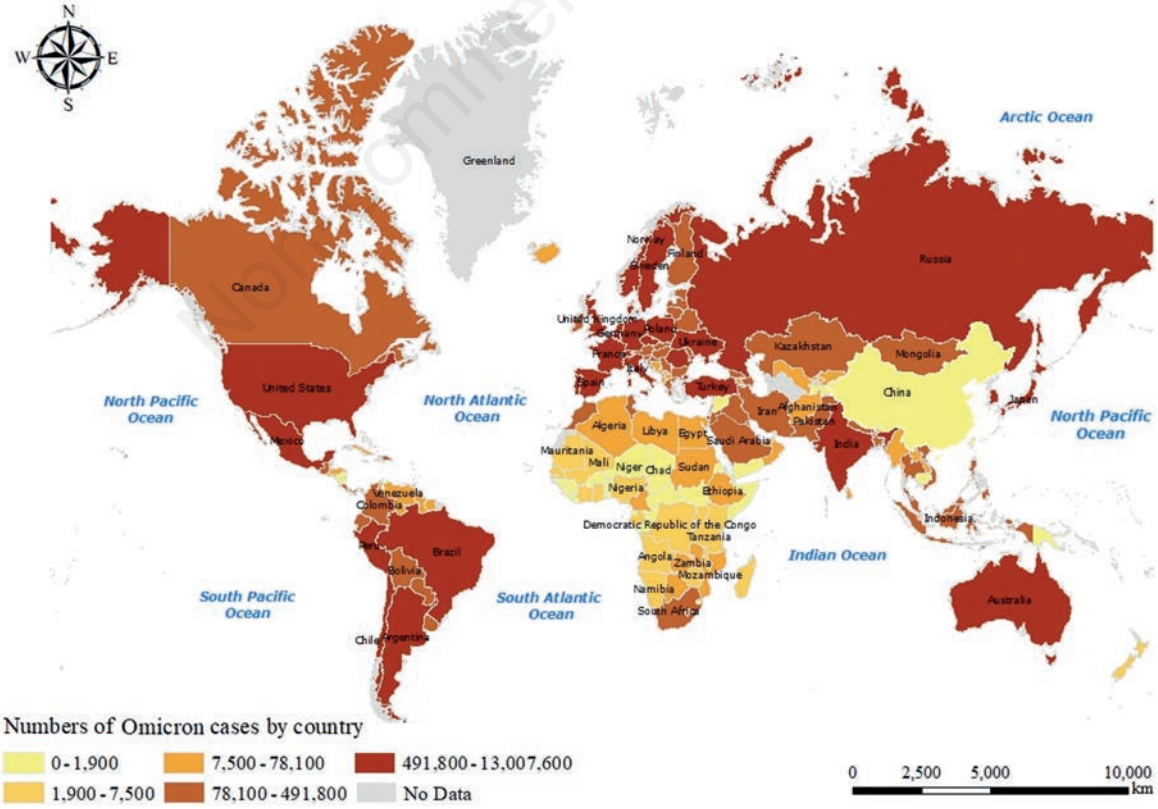

Figure 2. Total numbers of Omicron cases by country, presented as quintiles.

Denmark (19,360/100,000), Israel (17,487/100,000), Slovenia (13,455/100,000), Palau (12,277/100,000) and Netherlands (11,585/100,000) had the high-test incidence (Figure 3). In general, the case numbers and incidence in Africa were lower compared to all other continents, with Europe and Oceania showing much higher infection rates. Some countries had different ranks based on cases and incidence. For example, countries in North and South Africa, Russia, and India had the top 20% of the cases numbers but only the top 60% of incidence. Only three countries were without Omicron cases: Micronesia, Marshall Islands and Vanuatu.

Global spatial correlation analysis

Compared to Getis-Ord General G, Global Moran's *I* (Table 1) demonstrated a slight spatial autocorrelation of the Omicron variant worldwide among countries ($P<0.05$). A country's number of Omicron cases and incidence tended to be clustered together with that of its neighbours. The result of Getis-Ord General G (Table 1) further confirmed that high-value aggregations were more likely to appear ($P<0.01$).

Local spatial statistics

Overall, Getis-Ord Gi* identified 15 Omicron hotspots at three confidence levels (Table 2). Those with 99% confidence were observed in four continents: Asia (India), Europe (Germany, France, the United Kingdom and Italy), North America (USA), and South America (Brazil) (Figure 4). Minor (compared to the number of Europe hotspots) but still at significant confidence levels were seen in the Americas. No coldspot was recognized, and the remaining 177 countries were diagnosed as statistically non-significant.

Table 3 shows the 29 hotspots found at three confidence levels (identified by Getis-Ord Gi*). There were 17 hotspots at the 99% confidence level, all of which in Europe and Israel, so only the European part of the map is shown here (Figure 5). Oceania saw hotspots at more minor levels compared to Europe but still with statistical significance. No coldspot was recognized and the situation in the remaining 163 countries were statistically non-significant. Seven European countries were found both significantly hotspots in terms of cases and incidence, but significant level

Table 1. Global spatial clustering of Omicron case numbers and incidence.

Variable	Moran's *I* (Z score)	Getis-Ord General G (Z score)
Number of cases	0.065 (2.769)	0.012 (4.597)
Incidence	0.426 (14.504)	0.011 (12.740)

*Significant at the 99% confidence level.

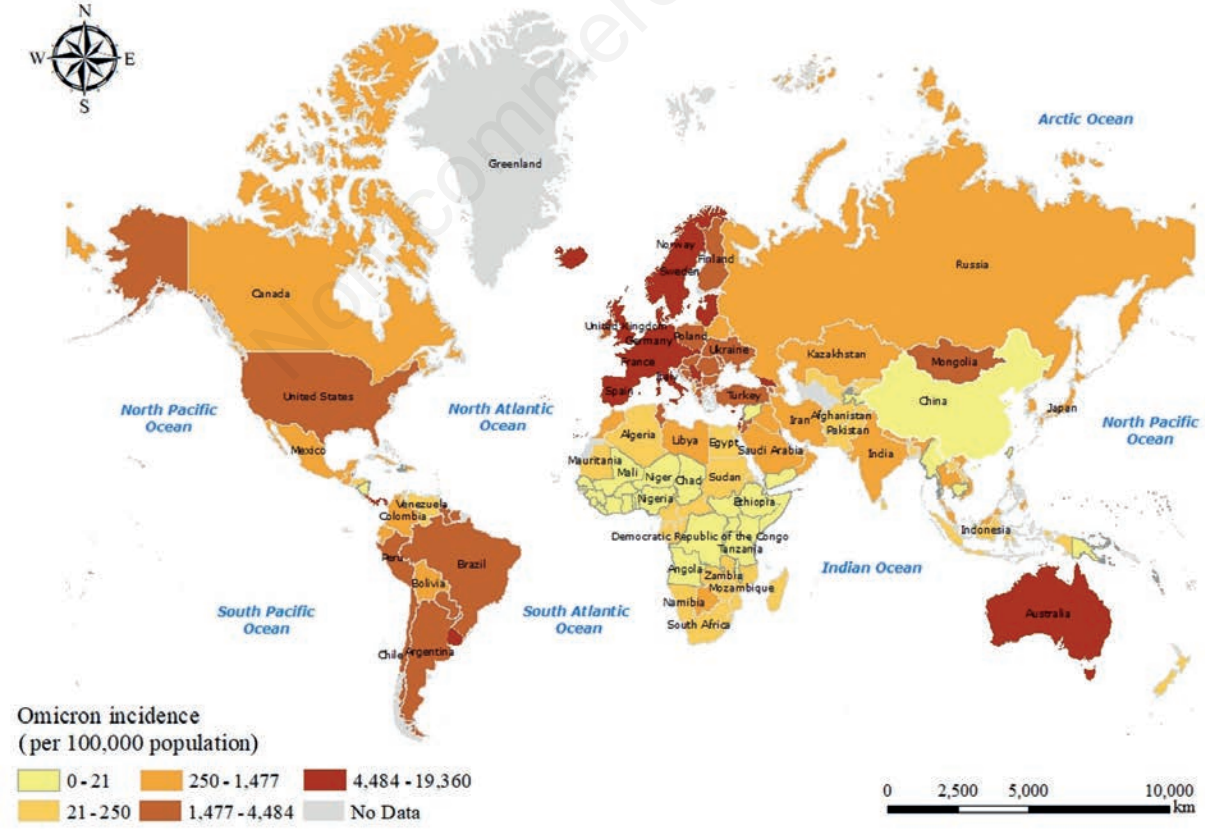

Figure 3. Omicron incidence (per 100,000 population) by country, presented as quintiles.

changed. Only Germany and France were both 99% significant hotspots for cases and incidence. The significance level of cases was higher than the incidence for Italy and Spain, while lower for Netherland, Belgium and Portugal.

From the perspective of Omicron cases, Local Moran's *I* identified 43 countries as significantly autocorrelated. The HH class included eight European countries and two North American ones (Figure 6), where Spain, France, the United Kingdom, Mexico, Netherlands, and Portugal were classified as HH clusters and hotspots. The LL clusters were all African countries and they

Table 2. Spatial distribution of Omicron cases and hotspots.

Country	Case number	Z score	P-value	Confidence level
Argentina	1,907,318	1.657	0.097	90%
Belgium	1,058,675	1.648	0.099	90%
Brazil	4,313,373	3.067	0.002	99%
Canada	490,916	1.692	0.091	90%
France	7,877,336	5.822	0	99%
Germany	4,201,627	3.197	0.001	99%
India	5,954,008	3.778	0	99%
Italy	3,767,986	2.611	0.009	95%
Mexico	934,232	2.191	0.028	95%
Portugal	1,250,944	1.770	0.077	90%
Spain	2,624,668	2.494	0.013	95%
The Netherlands	2,057,891	2.567	0.010	99%
United Kingdom	3,194,382	2.997	0.003	99%
USA	13,007,600	9.107	0	99%
Turkey	2,382,036	1.692	0.091	90%

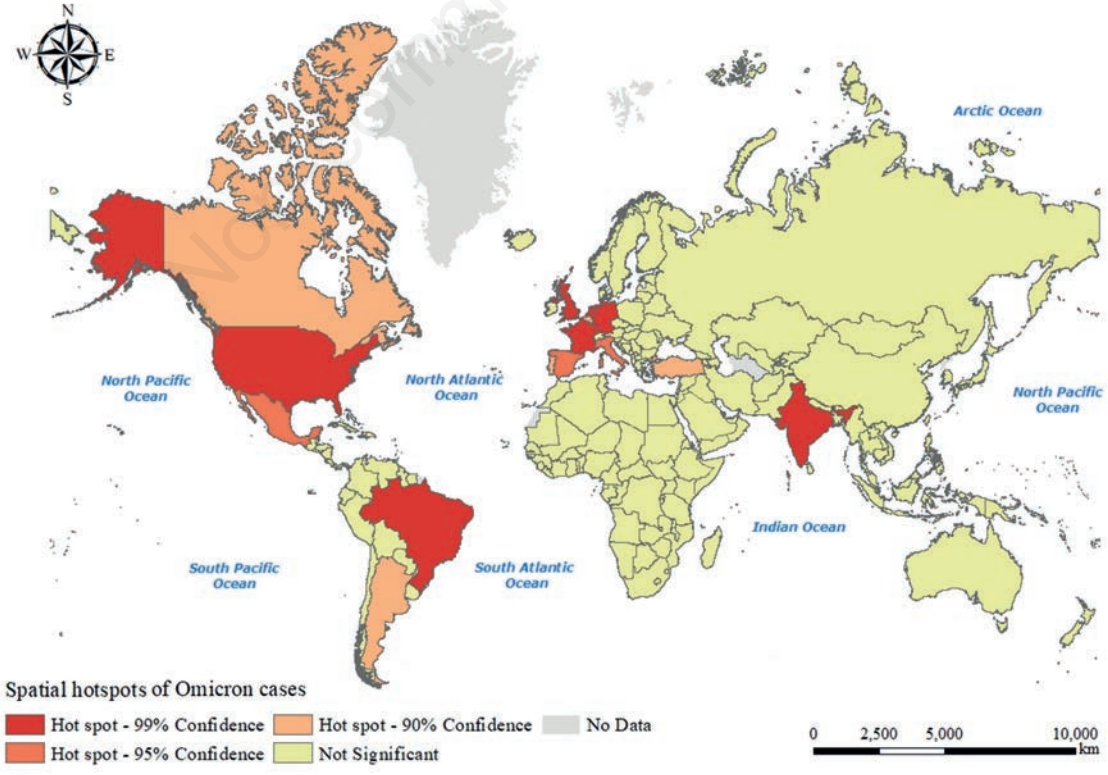

Figure 4. Spatial hotspots of Omicron cases.

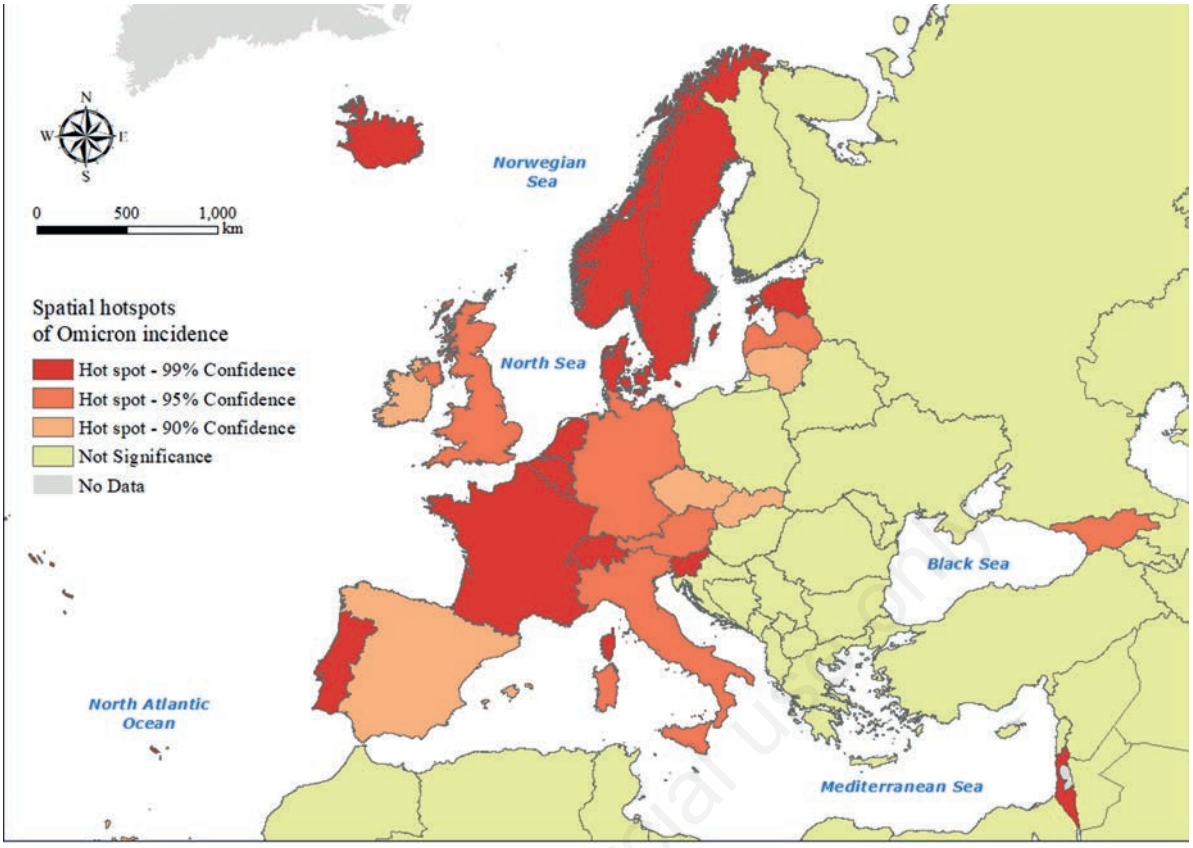

Figure 5. Spatial hotspots of Omicron incidence in Europe.

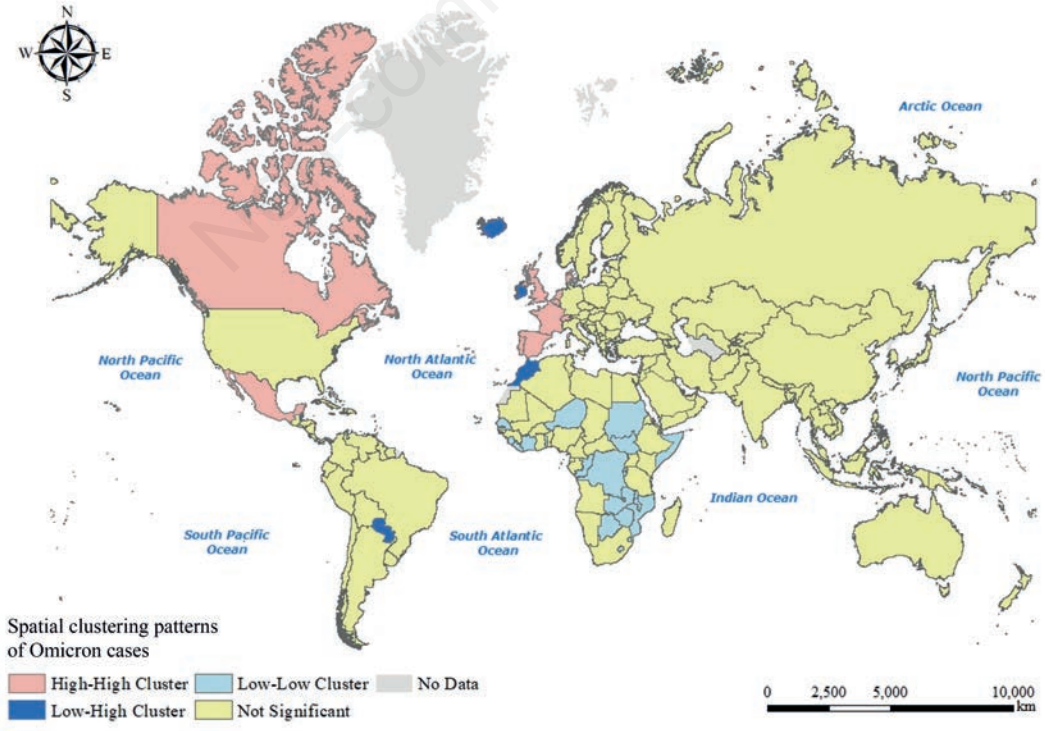

Figure 6. Spatial clustering patterns of Omicron cases.

almost covered the continent geographically. Only LH outliers were recognized and they were seen in 11 countries (Table 4). With exception of Paraguay, these countries were islands, close to the sea or a continental border.

From the perspective of Omicron incidence, Local Moran's *I* identified 98 countries as significantly autocorrelated. The HH class covered most of Europe, with Turkey the only HH country outside (Figure 7). The LL clusters (57 countries) were mainly identified in Asia, Africa and Pacific, with only four HL outliers dispersedly distributed in inland Asia, southeast Asia, eastern Africa and western Pacific (Table 5). The six LH outliers were identified in Europe, Middle East and north Africa.

Based on incidence, the pattern of spatial autocorrelation seems to be more informative. More HH and LL clusters were identified using incidence than based on the number of cases. Mexico and Canada, categorized as HH class of cases, and Comoros and Somalia categorized as LL, were not significantly recognized as clusters nor spatial outliers of incidence. Morocco was the only country classified as LH outlier from both incidence and cases number perspectives.

Discussion

With slightly positive spatial autocorrelation of global Omicron cases and incidence, we applied Global Moran's *I* and Getis-Ord General G to test the type of spatial autocorrelation, and the result claimed the existence of significant high-value clusters. Local Moran's *I* and Getis-Ord Gi* were calculated to locate the clusters and explore spatial outliers. Hotspots with significant confidence were identified in four (Asia, Europe, South America and North America) out of seven continents, which is of concern as many of these hotspots are connected and there is a high probability that they will eventually cause the dispersion of the Omicron variant worldwide.

Identifying spatial outliers may be more crucial than cluster detection for infectious diseases control. For example, Andorra, Ireland and Luxembourg have so far fewer Omicron variant cases, but they were surrounded by HH clusters at the time of our study, requiring extra protection strategies to avoid worse pandemic situations. Likewise, Belarus, Morocco and Syria were in a similar sit-

Table 3. Spatial distribution of Omicron incidence and hotspots.

Country	Incidence (per 100,000)	Z score	P-value	Confidence level
Andorra	19,360.00	6.176	0	99%
Austria	7,761.57	2.208	0.027	95%
Belgium	17,487.10	4.258	0	99%
Czech Republic	5,442.05	1.998	0.046	95%
Denmark	12,277.40	2.196	0.028	95%
Estonia	11,584.90	4.295	0	99%
France	11,305.50	3.162	0.002	99%
Georgia	6,482.69	1.839	0.066	90%
Germany	6,740.96	3.189	0.001	99%
Iceland	11,014.50	3.823	0	99%
Ireland	4,621.73	2.487	0.012	95%
Israel	10,735.80	3.780	0	99%
Italy	6,208.11	1.732	0.083	90%
Latvia	5,791.22	1.899	0.058	90%
Liechtenstein	10,269.50	2.176	0.030	95%
Lithuania	4,531.30	2.431	0.015	95%
Luxembourg	9,844.85	3.508	0	99%
Monaco	9,781.56	3.627	0	99%
Netherlands	9,592.73	2.662	0.008	99%
Norway	9,461.32	3.476	0	99%
Palau	5,743.77	2.194	0.028	95%
Portugal	8,988.20	3.727	0	99%
San Marino	8,558.58	3.647	0	99%
Slovakia	3,123.68	1.729	0.084	90%
Slovenia	8,280.99	3.796	0	99%
Spain	4,624.56	1.841	0.066	90%
Sweden	8,111.71	3.092	0.002	99%
Switzerland	13,455.20	3.843	0	99%
United Kingdom	6,545.22	3.342	0	99%

uation identified from the point of view of having a low incidence, while the countries closest to them had high values. The reason might be due to various reasons, such as not having numerous airline connections or not sharing borders with many countries; for islands none at all. The threat might thus be less than being surrounded by hotspots; however, they still need to be alerted to prevent further spread of the highly infectious variants, such as the Omicron.

This study used a combined spatial weight matrix to include air travel connectivity in the spatial relationships among countries.

Table 4. Omicron cases by country and their spatial clustering patterns.

Country	Cases no.	Local Moran's *I*	P-value	Clustering type
Andorra	8,175	–0.379	0.006	LH
Bahamas	2,963	–0.378	0.02	LH
Belgium	1,058,675	0.571	0.006	HH
Belize	15,083	–0.298	0.028	LH
Botswana	21,977	0.095	0.042	LL
Burundi	1,701	0.100	0.022	LL
Canada	490,916	0.060	0.002	HH
Comoros	274	0.105	0.004	LL
Côte d'Ivoire	2,545	0.106	0.002	LL
Democratic Republic of the Congo	4,024	0.105	0.002	LL
Denmark	1,140,167	0.375	0.044	HH
France	7,877,336	2.789	0.046	HH
Iceland	40,174	–0.512	0.002	LH
Ireland	175,072	–0.299	0.008	LH
Jamacia	18,548	–0.202	0.048	LH
Lesotho	768	0.099	0.036	LL
Liberia	237	0.100	0.026	LL
Luxembourg	51,265	–0.393	0.004	LH
Malawi	3,046	0.104	0.002	LL
Mexico	934,232	0.708	0.01	HH
Morocco	126,516	–0.265	0.012	LH
Mozambique	8,000	0.097	0.016	LL
Netherlands	2,057,891	1.756	0.008	HH
Niger	397	0.102	0.008	LL
Paraguay	133,366	–0.140	0.048	LH
Portugal	1,250,944	0.744	0.014	HH
Republic of Congo	1,442	0.106	0.004	LL
Samoa	30	–0.299	0.018	LH
São Tomé and Príncipe	512	0.106	0.002	LL
Senegal	3,942	0.106	0.002	LL
Sierra Leone	148	0.100	0.018	LL
Somalia	1,942	0.104	0.002	LL
South Sudan	473	0.105	0.004	LL
Spain	2,624,668	1.558	0.014	HH
Sudan	9,539	0.096	0.008	LL
Swaziland	1,051	0.102	0.018	LL
Switzerland	881,248	0.436	0.004	HH
Togo	1,195	0.106	0.002	LL
Tonga	65	–0.249	0.044	LH
United Kingdom	3,194,382	2.168	0.008	HH
Zambia	16,974	0.099	0.006	LL
Zimbabwe	5,956	0.099	0.008	LL

HH, High-High cluster; LH, Low-High cluster; LL, Low-Low cluster.

Studies have verified air travel networks' vital role in building spatial relationships while studying disease transmission (Bogoch *et al.,* 2015; Zaki *et al.,* 2012; Sun *et al.,* 2021). Restrictions on international air travel have been found to cut transmission at the regional level, especially at the early stage, which can be essential for controlling pandemics (Kraemer *et al.,* 2020). The challenge is how to develop an adaptive spatial weight matrix framework to respond to changing international travel bans. Changing a country's decision to close borders or lockdown can drastically affect neighbouring countries (Krisztin *et al.,* 2020). Meanwhile, further investigation on the transmission path is needed as the Omicron variant spreads faster and easier than the previous SARS-CoV-2 variants (He *et al*., 2021). This character may require multi-source traffic information to build spatial weight matrix, such as cross-border logistics routes.

There are some limitations in this study concerning the data used. The first is the uncertainties regarding the number of Omicron cases. The values used in this study were calculated by multiplying the genomic rate and the number of new confirmed COVID-19 cases submitted by each country. The observed frequency varies among countries. Meanwhile, many middle- and low-income countries do not have strong health systems and under-reporting of the number of cases is inevitable. The second limitation is the unequal time lag between sample collection and submission. Due to the inevitable differences between counties, it is difficult to require all the countries to reach the same standard in terms of time lag. The differences in the time for delivering samples to laboratories, analyzing, and uploading sequence to GISAID can result in biased submission data (Kalia *et al*., 2021). Though the GISAID website claims the data summarized do not represent exact prevalence, it remains of great value as the largest open-access portal for collecting SARS-CoV-2 strains data from gaining access worldwide. In addition, due to the limitation of data, we cannot precisely discern whether we referred to a connecting flight or a direct flight. Some countries, *e.g*., Qatar and Dubai, are airline hubs and many passengers change flights in these countries. How to deal with the population connectivity in these countries still needs further study.

A global tracking system is needed to keep countries updated on the spatial spread of the Omicron variant so that the governments can adjust their national and international pandemic prevention policies. The total cases of the Omicron variant and its spatial pattern reveal the current stage of challenge the world needs to meet. The increasing speed and the transmission rate of the Omicron variant also require attention to prepare for future problems. It is an important but challenging goal for all countries to report newly increased cases timely and accurately. The coordination of global health organizations, such as the WHO, may need to offer aid to those countries lacking sufficient medical resources. Hopefully, every country can learn from the experience with COVID-19 and work together to end the pandemic soon.

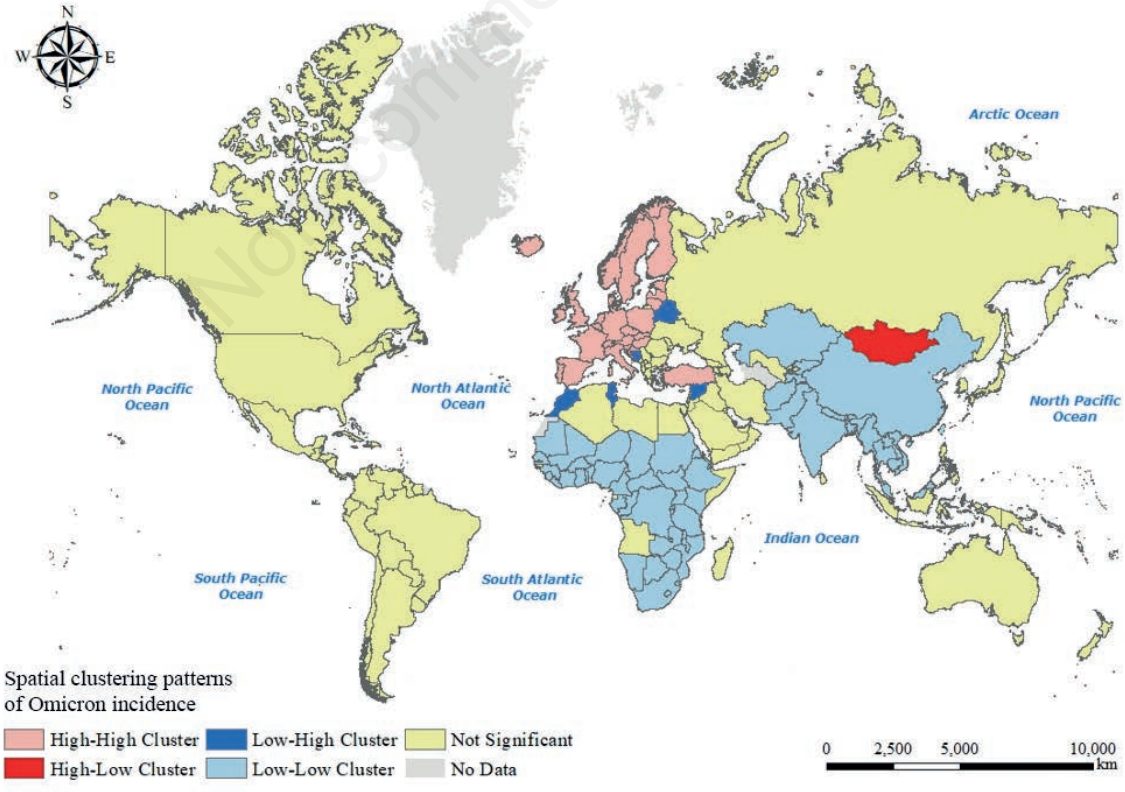

Figure 7. Spatial clustering patterns of Omicron incidence.

Table 5. Omicron incidence by country and their spatial clustering patterns.

Country	Incidence per 100,000	Local Moran's *I*	P-value	Type
Afghanistan	30.85	0.337	0.028	LL
Andorra	6,545.00	1.945	0.002	HH
Austria	5,442.05	1.050	0.002	HH
Bangladesh	163.82	0.368	0.002	LL
Belarus	934.60	–0.245	0.04	LH
Belgium	8,988.20	3.719	0.002	HH
Benin	3.46	0.409	0.002	LL
Bhutan	397.21	0.342	0.01	LL
Bosnia and Herzegovina	1,526.08	–0.151	0.046	LH
Botswana	915.34	0.266	0.004	LL
Brunei	714.67	0.226	0.044	LL
Burkina Faso	3.09	0.383	0.002	LL
Burundi	14.58	0.415	0.004	LL
Cambodia	7.85	0.331	0.022	LL
Cameroon	27.64	0.350	0.008	LL
Central African Republic	26.34	0.395	0.004	LL
Chad	3.86	0.321	0.038	LL
China	0.13	0.294	0.034	LL
Côte d'Ivoire	9.35	0.450	0.002	LL
Croatia	3,691.25	0.431	0.004	HH
Czech Republic	6,482.69	0.852	0.022	HH
Democratic Republic of the Congo	3.43	0.447	0.002	LL
Denmark	19,360.00	7.368	0.002	HH
Djibouti	73.58	0.337	0.014	LL
Eritrea	21.03	0.407	0.006	LL
Estonia	9,592.73	1.434	0.024	HH
Ethiopia	13.15	0.389	0.002	LL
Finland	3,249.11	0.265	0.006	HH
France	11,014.50	3.647	0.002	HH
Gabon	83.56	0.358	0.008	LL
Gambia	32.04	0.308	0.042	LL
Germany	4,531.30	1.180	0.002	HH
Ghana	14.88	0.348	0.008	LL
Guinea	8.77	0.377	0.012	LL
Hungary	3,909.71	0.394	0.008	HH
Iceland	10,735.80	3.643	0.002	HH
India	332.42	0.314	0.004	LL
Ireland	3,123.68	0.353	0.002	HH
Italy	5,743.77	1.257	0.002	HH
Kazakhstan	1,260.45	0.141	0.024	LL
Kenya	11.78	0.393	0.004	LL
Kyrgyzstan	186.72	0.324	0.016	LL
Laos	179.62	0.319	0.034	LL
Latvia	7,761.57	1.142	0.024	HH
Lesotho	39.97	0.413	0.01	LL
Liberia	5.14	0.436	0.002	LL
Liechtenstein	8,280.99	2.767	0.002	HH
Lithuania	6,208.11	0.761	0.02	HH
Luxembourg	8,558.58	3.559	0.002	HH
Malawi	16.07	0.441	0.002	LL

To be continued on next page

Table 5. Continued from previous page.

Country	Incidence per 100,000	Local Moran's *I*	P-value	Clustering type
Luxembourg	8,558.58	3.559	0.002	HH
Malawi	16.07	0.441	0.002	LL
Malaysia	464.18	0.250	0.044	LL
Mali	10.87	0.401	0.004	LL
Mauritania	125.95	0.346	0.012	LL
Monaco	6,740.96	1.855	0.004	HH
Mongolia	4,080.20	–0.260	0.04	HL
Morocco	345.85	–0.419	0.03	LH
Mozambique	25.92	0.393	0.01	LL
Myanmar	16.41	0.404	0.006	LL
Namibia	117.98	0.381	0.01	LL
Nepal	318.98	0.352	0.002	LL
Netherlands	11,584.90	4.785	0.002	HH
Niger	1.61	0.424	0.006	LL
Nigeria	1.74	0.362	0.002	LL
Norway	9,461.32	3.205	0.002	HH
Pakistan	69.99	0.359	0.002	LL
Palau	12,277.40	–1.610	0.002	HL
Poland	2,401.03	0.018	0.002	HH
Portugal	11,305.50	1.839	0.034	HH
Republic of Congo	34.76	0.435	0.002	LL
Rwanda	38.43	0.438	0.002	LL
San Marino	9,781.56	2.637	0.004	HH
São Tomé and Príncipe	253.25	0.399	0.002	LL
Senegal	16.92	0.431	0.006	LL
Seychelles	7,480.22	–0.830	0.006	HL
Sierra Leone	2.13	0.437	0.002	LL
Singapore	3,229.38	–0.140	0.008	HL
Slovakia	5,791.22	0.990	0.012	HH
Slovenia	13,455.20	2.476	0.012	HH
South Africa	144.13	0.353	0.004	LL
South Sudan	2.75	0.445	0.002	LL
Spain	4,624.56	0.818	0.002	HH
Sudan	21.76	0.422	0.002	LL
Swaziland	93.22	0.403	0.004	LL
Sweden	8,111.71	2.567	0.002	HH
Switzerland	9,844.85	3.195	0.002	HH
Syria	5.80	–0.447	0.04	LH
Tajikistan	2.45	0.349	0.022	LL
Tanzania	4.97	0.405	0.002	LL
Thailand	291.39	0.275	0.042	LL
Togo	13.33	0.443	0.002	LL
Tunisia	1,644.82	–0.120	0.042	LH
Turkey	2,803.91	0.101	0.014	HH
Uganda	13.52	0.435	0.002	LL
United Kingdom	4,621.73	1.255	0.002	HH
Vatican City	51.11	–0.848	0.002	LH
Vietnam	250.67	0.289	0.032	LL
Zambia	88.45	0.413	0.002	LL
Zimbabwe	40.39	0.414	0.004	LL

HH, High-High cluster; HL, High-Low cluster; LH, Low-High; LL, Low-Low cluster.

Conclusions

The Omicron variant poses a severe threat to the health of all global citizens. A complete picture of the spatial distribution of Omicron cases can help set strategies with neighbour countries to fight the virus together. This study applied spatial statistics methods at the country level identifying general pattern of high-value clusters in four continents. Different but vital controlling approaches are needed to stop further spread of the Omicron variant, in particular outliers next to countries with many hotspots in Europe. It is a strong need to alert and guard against possible new virus invasions.

References

Alkhatib M, Svicher V, Salpini R, Ambrosio FA, Bellocchi MC, Carioti L, Piermatteo L, Scutari R, Costa G, Artese A, Alcaro S, Shafer R, Ceccherini-Silberstein F, 2021. SARS-CoV-2 Variants and their relevant mutational profiles: update summer 2021. Microbiol Spectr 9:e109621.

Anselin L, 2010. Local indicators of spatial association-LISA. Geogr Anal 27:93-115.

Bisanzio D, Kraemer MUG, Bogoch II, Brewer T, Brownstein JS, Reithinger R, 2020. Use of Twitter social media activity as a proxy for human mobility to predict the spatiotemporal spread of COVID-19 at global scale. Geospat Health 15:19-24.

Bogoch II, Creatore MI, Cetron MS, Brownstein JS, Pesik N, Miniota J, Tam T, Hu W, Nicolucci A, Ahmed S, Yoon JW, Berry I, Hay SI, Anema A, Tatem AJ, MacFadden D, German M, Khan K, 2015. Assessment of the potential for international dissemination of Ebola virus via commercial air travel during the 2014 West African outbreak. Lancet 385:29-35.

Callaway E, 2021. Heavily mutated Omicron variant puts scientists on alert. Nature 600:21.

Case AC, Rosen HS, Hines JR, 1993. Budget spillovers and fiscal policy interdependence: evidence from the states. J Public Econ 52:285-307.

CDC, 2021. Science Brief: Omicron (B.1.1.529) Variant | CDC, (n.d.). Available from: https://www.cdc.gov/coronavirus/2019-ncov/science/science-briefs/scientific-brief-omicron-variant.html Accessed: 9 December 2021.

Chen J, Wang R, Gilby NB, Wei G, 2022. Omicron Variant (B.1.1.529): infectivity, vaccine breakthrough, and antibody resistance. J Chem Inf Model 62:412-22.

Franch-Pardo I, Napoletano B M, Rosete-Verges F, Billa L, 2020. Spatial analysis and GIS in the study of COVID-19. A review. Sci Total Environ 739:140033.

Findlater A, Bogoch II, 2018. Human mobility and the global spread of infectious diseases: a focus on air travel. Trends Parasitol 34:772-83.

Fix E, Hodges JL, 1951. Discriminatory analysis. Nonparametric discrimination: consistency properties. USAF School of Aviation Medicine, Randolph Field, Texas. Project no. 21-49-004, report no. 4. Available from: https://apps.dtic.mil/dtic/tr/fulltext/u2/a800276.pdf

Getis A, Ord JK, 2010. The analysis of spatial association by use of distance statistics. Geogr Anal 24:189-206.

GISAID, 2022 Tracking of variants. GISAID. 2022. Available from: https://www.gisaid.org/hcov19-variants/ Accessed: 10 February 2022.

Gushulak BD, MacPherson DW, 2000. Population mobility and infectious diseases: The diminishing impact of classical infectious diseases and new approaches for the 21st century. Clin Infect Dis 31:776-80.

He X, Hong W, Pan X, Lu G, Wei X, 2021. SARS-CoV-2 Omicron variant: characteristics and prevention. MedComm 2:838-45.

Huang Y, Yang S, Zou Y, Su J, Wu C, Zhong B, Jia P, 2022. Spatiotemporal epidemiology of COVID-19 from an epidemic course perspective. Geospat Health 17(s1):1023.

Islam A, Sayeed MA, Rahman MK, Ferdous J, Islam S, Hassan MM, 2021. Geospatial dynamics of COVID-19 clusters and hotspots in Bangladesh. Transbound Emerg Dis 68:3643-57.

Kalia K, Saberwal G, Sharma G, 2021. The lag in SARS-CoV-2 genome submissions to GISAID. Nat Biotechnol 39:1058-60.

Kannan SR, Spratt AN, Sharma K, Chand HS, Byrareddy SN, Singh, K, 2022. Omicron SARS-CoV-2 variant: unique features and their impact on pre-existing antibodies. J Autoimmun 126:102779.

Kooijman SALM, 1976. Some remarks on the statistical analysis of grids especially with respect to ecology. Ann Syst Res 5:113-32.

Kraemer MUG, Yang C-H, Gutierrez B, Wu C-H, Klein B, Pigott DM, Open COVID-19 Data Working Group, du Plessis L, Faria NR, Li R, Hanage WP, Brownstein JS, Layan M, Vespignani A, Tian H, Dye C, Pybus OG, Scarpino SV, 2020. The effect of human mobility and control measures on the COVID-19 epidemic in China. Science 368:493-7.

Krisztin T, Piribauer P, Wögerer M, 2020. The spatial econometrics of the coronavirus pandemic. Lett Spat Resour Sci 13:209-18.

Li H, Li H, Ding Z, Hu Z, Chen F, Wang K, Peng Z, Shen H, 2020. Spatial statistical analysis of coronavirus disease 2019 (covid-19) in China. Geospat Health 15:867.

Moran PAP, 1950. Notes on continuous stochastic phenomena. Biometrika 371:17-23.

Ping J, Green C, Zartman R, Bronson K, 2004. Exploring spatial dependence of cotton yield using global and local autocorrelation statistics. Field Crops Res 89:219-36.

Sun X, Wandelt S, Zhang A, 2021. On the degree of synchronization between air transport connectivity and COVID-19 cases at worldwide level. Transport Policy 105:115-23.

Tiecco G, Storti S, Degli Antoni M, Foca E, Castelli F, Quiros-Roldan E, 2022. Omicron genetic and clinical peculiarities that may overturn SARS-CoV-2 pandemic: a literature review. Int J Mol Sci 23:1987.

Wang W, Tang J, Wei F, 2020. Updated understanding of the outbreak of 2019 novel coronavirus (2019□nCoV) in Wuhan, China. J Med Virol 92:441-7.

Zaki AM, van Boheemen S, Bestebroer TM, Osterhaus ADME, Fouchier RA M, 2012. Isolation of a Novel Coronavirus from a Man with Pneumonia in Saudi Arabia. N Engl J Med 367:1814-20.

Zhang L, Li Q, Liang Z, Li T, Liu S, Cui Q, Nie J, Wu Q, Qu X, Huang W, Wang Y, 2022. The significant immune escape of pseudotyped SARS-CoV-2 variant Omicron. Emerg Microbes Infec 11:1-5.